

Limits on the Gravitational Wave Background from Spacecraft Doppler Experiments

GIACOMO GIAMPIERI^{1,2} & ALBERTO VECCHIO²

¹ *Jet Propulsion Laboratory, California Institute of Technology,
MS 301-150, 4800 Oak Grove Drive - Pasadena, CA 91109 - USA.*

² *Dipartimento di Fisica Nucleare e Teorica, Università di Pavia, Via Bassi 6 - 27100 Pavia - Italy.*

April 29, 1994

Abstract

Doppler tracking of an interplanetary spacecraft provides an unique opportunity to search for low frequency gravitational waves. In this paper, we describe in detail how Doppler experiments can be used to set an upper limit on a stochastic gravitational background, isotropically distributed. After reviewing the basic equations involved in this technique, we analyze, in a critical way, three methods of data analysis, based on different assumptions about the physical properties of the signal.

1 Introduction

Besides the most studied sources of gravitational radiation, usually classified in burst sources (e.g. supernovae) and continuous sources (e.g. binaries), One can explore the possibility that the universe is filled with a gravitational background. Various possible background sources have been suggested, ranging from a random superposition of periodic signals from binary systems, to quantum fluctuations of the primordial universe. Of special interest, considering the recent COBE results, are the relic gravitational waves (GW) produced during inflation. However, independently of its origin, the principal characteristic of this signal is its continuous and stochastic nature. In fact, from the observational point of view, the distinction between primordial and generated background is irrelevant: we can only determine the values of ρ_g (energy density of the

background) and ω (its characteristic frequency) for which the background becomes observable, with an experiment based on the Doppler tracking of an interplanetary spacecraft.

In these experiments, the Earth and the spacecraft are used as free end-points of a low frequency GW detector. A radio link is transmitted from the Earth to the spacecraft, coherently transponded and sent back to the Earth, where its frequency is measured with great accuracy. Comparing the emitted and received frequency, one can determine the Doppler shift $\Delta\nu/\nu_0$ (where ν_0 is the nominal frequency and $\Delta\nu$ its variation) as a function of time. This Doppler shift is mainly due to the orbital motion, and, secondarily, to a rather long series of noises. In addition, as shown by Estabrook and Wahlquist (1975), the theoretical Doppler sequence is also affected, with a characteristic three-pulse response, by a gravitational wave possibly passing by.

In the following section, we will summarize how a GW background, assumed to be isotropic, contributes to the power spectrum of the Doppler signal. In §3 we will study the corresponding autocorrelation function generated by such a background. In §4 we will analyze the consequences of the additional assumption that the power spectrum of the GW amplitude is given by a power law, focussing our attention to two important values of the spectral slope. Finally, in §5 we consider three different techniques for the data analysis. Two of these methods, previously applied to real data, are reanalyzed in great detail, while the third one is new, having been used for the first time in the *Ulysses* GW experiment, whose results are reported in Bertotti *et al.* (1994).

2 Power Spectrum of the Doppler Signal

Gravitational waves can be described as strain waves which propagate at the speed of light through the space and are represented by a dimensionless 4-tensor $h_{\alpha\beta}$ giving the perturbation of the metric. In the linearized theory and in the gauge TT (Transverse and Traceless) for a wave which propagates in the z -direction, $h_{\alpha\beta}$ can be written in

terms of the two polarization amplitudes h_+ and h_\times as

$$h_{\alpha\beta} = \begin{bmatrix} 0 & 0 & 0 & 0 & 0 \\ 0 & h_+ & h_\times & h_\times & 0 \\ 0 & h h_\times & -h h_+ & 0 & 0 \\ 0 & 0 & 0 & 0 & 0 \end{bmatrix}. \quad (2.1)$$

The Doppler effect $y_{\hat{k}}(t) = \Delta\nu/\nu_0$ produced by a linearized gravitational plane wave $h_{\alpha\beta}$ on the monochromatic electromagnetic signal, of frequency ν_0 , propagating along the direction $\hat{k} = (\sin\theta\cos\phi, \sin\theta\sin\phi, \cos\theta)$ from the Earth to the spacecraft, transponded and then transmitted back to the Earth is given by (Estabrook & Wahlquist 1975)

$$y_{\hat{k}}(t) = - (1 - \mu)h(t) - 2\mu h(t - \ell - \ell\mu) - (1 + \mu)h(t - 2\ell), \quad (2.2)$$

where ℓ is half of the Round Trip Light Time (RTLT), and where we have defined

$$h \equiv \frac{1}{2}(h_+ \cos 2\phi + h_\times \sin 2\phi),$$

$$\mu \equiv \cos\theta.$$

We assume that the gravitational field is observed for a time T_1 , and we introduce the Fourier transforms

$$h_p(t) \equiv \frac{T_1^{1/2}}{2\pi} \int_{-\infty}^{+\infty} d\omega \tilde{h}_p(\omega) e^{i\omega t}, \quad (2.3)$$

where p stands for $+$ and \times . The $T_1^{1/2}$ normalization has been introduced since a rigorous definition of the Fourier spectral density needs a continuous and infinite ($T_1 \rightarrow \infty$) sample, which is obviously unreachable in a real experiment.

We define the mean squared amplitude of the gravitational background as

$$\langle h^2 \rangle \equiv \frac{1}{T_1} \int_{-T_1/2}^{+T_1/2} dt \left[h_+(t)^2 + h_\times(t)^2 \right] = \frac{1}{\pi} \int_0^\infty d\omega S_h(\omega). \quad (2.4)$$

where $S_h(\omega) \equiv |\hat{h}_+(\omega)|^2 + |\hat{h}_\times(\omega)|^2$ is the amplitude spectral density. We also introduce the energy spectral density $S_\rho(\omega)$ via the energy density of the gravitational background

$$\rho_g = \frac{1}{\pi} \int_0^\infty d\omega S_\rho(\omega). \quad (2.5)$$

Since the GW energy density is also given by the Isaacson formula (Isaacson 1968)

$$\rho_g = \frac{1}{16\pi^2} \int_0^\infty d\omega \omega^2 S_h(\omega), \quad (2.6)$$

then comparing equations (2.5) and (2.6) we obtain

$$S_\rho(\omega) = \frac{1}{16\pi} \omega^2 S_h(\omega). \quad (2.7)$$

We want to relate the spectral energy density $S_\rho(\omega)$ to an observable quantity, i.e. the spectral density of the Doppler signal $S_y(\omega)$.

Squaring equation (2.2) and averaging over the observing time T_1 , we get the average power coming from the given direction (θ, ϕ)

$$\begin{aligned} \langle y_k^2 \rangle_t &= \frac{1}{T_1} \int_{-T_1/2}^{+T_1/2} dt |y_k(t)|^2 \\ &= \frac{1}{2\pi} \int_{-\infty}^{+\infty} d\omega |h_+ \cos(2\phi) + h_\times \sin(2\phi)|^2 \left[\mu^2 + \sin^2(\omega\ell) \right. \\ &\quad \left. + \mu^2 \cos^2(\omega\ell) - 2\mu \sin(\omega\ell) \sin(\mu\omega\ell) - 2\mu^2 \cos(\omega\ell) \cos(\mu\omega\ell) \right]. \end{aligned} \quad (2.8)$$

For an isotropic background, the waves come from all the directions with, statistically, the same amplitude. Therefore, the total average power is

$$\langle y^2 \rangle = \frac{1}{4\pi} \int_0^{2\pi} d\phi \int_{-1}^{+1} d\mu \langle y_k^2 \rangle_t = \frac{1}{4\pi} \int_{-\infty}^{+\infty} d\omega S_h(\omega) \mathbf{R}(\omega\ell), \quad (2.9)$$

where $\mathbf{R}(\omega l)$ is the transfer function given by

$$\mathbf{R}(x) = \frac{x^2 - 3}{x^2} - \frac{x^2 + 3}{3x^2} \cos(2x) + \frac{2}{x^3} \sin(2x). \quad (2.10)$$

The function $\mathbf{R}(x)$ has the following asymptotic behaviour

$$\mathbf{R}(x) = 1 - \frac{1}{3} \cos x - \mathcal{O}\left(\frac{1}{x^2}\right) \quad \text{for } x \gg 1, \quad (2.11)$$

and

$$\mathbf{R}(x) = \frac{8}{15} x^2 + \mathcal{O}(x^4) \quad \text{for } x \ll 1 \quad (2.12)$$

Now we can define the spectral power of the Doppler signal as

$$\langle y^2 \rangle = \frac{1}{\pi} \int_0^\infty d\omega S_y(\omega). \quad (2.13)$$

From equations (2.7), (2.9), and (2.13) we have the following relations between the basic spectral quantities

$$S_y(\omega) = \frac{1}{2} \mathbf{R}(\omega l) S_h(\omega) = \frac{8\pi}{\omega^2} \mathbf{R}(\omega l) S_\rho(\omega). \quad (2.14)$$

3 Autocovariance Function of the Doppler Signal

The autocovariance function of the GW amplitude is defined as

$$H(t) \equiv \frac{1}{T_1} \int_{-T_1/2}^{+T_1/2} dt' h(t') h(t + t'). \quad (3.1)$$

The autocovariance function of the Doppler signal y_k is therefore

$$\begin{aligned}
C_k(t) &\equiv \frac{1}{T_1} \int_{-T_1/2}^{+T_1/2} dt' y_k(t') y_k(t + t') \\
&= (2 + 6\mu^2)H(t) + (1 - \mu^2)[H(t - 2\ell) + H(t + 2\ell)] \\
&\quad + 2\mu(1 - \mu)[H(t - \ell + \ell\mu) + H(t - \ell - \ell\mu)] \\
&\quad + 2\mu(1 + \mu)[H(t + \ell - \ell\mu) + H(t + \ell + \ell\mu)] .
\end{aligned} \tag{3.2}$$

The average over the solid angle gives the theoretical autocovariance function $C(t)$

$$C(t) = \frac{1}{4\pi} \int_0^{2\pi} d\phi \int_{-1}^{+1} d\mu C_k(t) . \tag{3.3}$$

With our assumption of isotropy, the average over ϕ gives terms of the form

$$\langle H(t) \rangle_\phi \equiv \frac{1}{2\pi} \int_0^{2\pi} d\phi H(t) = \frac{1}{8\pi} \int_0^\infty d\omega S_h(\omega) \cos \omega t , \tag{3.4}$$

which for $t = 0$ reads

$$\langle H(0) \rangle_\phi = \frac{1}{8} \langle h^2 \rangle . \tag{3.5}$$

Finally, when the average over μ is performed we get

$$C(t) = 4 \left[\langle H(t) \rangle_\phi + \frac{1}{6} \langle H(t - 2\ell) \rangle_\phi + \frac{1}{6} \langle H(t + 2\ell) \rangle_\phi + \frac{1}{4} I(t) \right] , \tag{3.6}$$

where $I(t)$ comes from the terms in equation (3.2) with μ -dependence on the argument of H :

$$I(t) = \int_{-1}^{+1} d\mu \left\{ \mu(1-\mu) [\langle H(t+\ell+\ell\mu) \rangle_\phi + \langle H(t-\ell-\ell\mu) \rangle_\phi] \right. \\ \left. - \mu(1+\mu) [\langle H(t-\ell-\ell\mu) \rangle_\phi - \langle H(t+\ell+\ell\mu) \rangle_\phi] \right\}. \quad (3.7)$$

We may rewrite equation (3.7), using the spectral decomposition given in equation (2.4), as

$$I(t) = \frac{1}{4\pi} \int_0^\infty d\omega S_h(\omega) \mathbf{I}(\omega\ell) \cos \omega t, \quad (3.8)$$

where

$$\mathbf{I}(\omega\ell) = \int_{-1}^{+1} d\mu \left\{ \mu(1-\mu) \cos[\omega\ell(1+\mu)] - \mu(1+\mu) \cos[\omega\ell(1-\mu)] \right\} \\ = -\frac{6}{(\omega\ell)^2} - \frac{2 \cos 2\omega\ell}{(\omega\ell)^2} + \frac{4 \sin 2\omega\ell}{(\omega\ell)^3}.$$

From equations (2.14), (3.4), (3.6) and (3.8) we can find the Wiener-Khintchin theorem, relating the autocovariance function and the power spectrum of the Doppler signal:

$$C(t) = \frac{1}{2\pi} \int_0^\infty d\omega S_h(\omega) \left[1 - \frac{1}{3} \cos 2\omega\ell \right. \\ \left. - \frac{3}{(\omega\ell)^2} - \frac{\cos 2\omega\ell}{(\omega\ell)^2} + \frac{2 \sin 2\omega\ell}{(\omega\ell)^3} \right] \cos \omega t \\ \left. - \frac{1}{2\pi} \int_0^\infty d\omega \left\{ S_x(\omega) \mathbf{I}(\omega\ell) \cos \omega t - \frac{1}{\pi} \int_0^\infty d\omega' S_y(\omega') \cos \omega' t \right\} \right]. \quad (3.9)$$

4 The Spectrum of the Gravitational Background

The basic problem for detection experiments is the presence of noise, which in the case of interplanetary spacecraft Doppler tracking dominates the expected gravitational signal. Therefore, our aim is to set an upper limit on the total energy density associated with the GW background, or, equivalently, to its energy flux. This limit will be significant, from a cosmological point of view, if it will be comparable to the critical value $\rho_c = 3H_0^2/8\pi$ (where H_0 is the present value of the Hubble parameter), corresponding to a (pseudo-)euclidean Universe.

Several theoretical constraints can be put on the density parameter $\Omega_g \equiv \rho_g/\rho_c$ of the background, once a particular cosmological model is chosen (Carr 1980, updated in Giampieri 1992). The most stringent one, at least in the standard model, comes from nucleosynthesis arguments: in fact, in order to keep the helium production at an acceptable value, Ω_g must not be higher than the electromagnetic density parameter $\Omega_{em} \simeq 10^{-4}$. Since this limit applies only to a primordial (i. e., already present at the nucleosynthesis epoch) background, an important target of current experiments is the gravitational background generated astrophysically after the nucleosynthesis.

From the experimental point of view, on the other side, various upper limit to $S_\rho(\omega)$ have been established; the most stringent limits are those, at $\omega \approx 10^{-8}$ Hz, from the irregularities in the period of fast pulsars. However, in the mHz band the Doppler method is the only one available at the present time.

It can be shown that, in order of magnitude, a gravitational background of dimensionless amplitude h and characteristic (present) period P corresponds to a density parameter

$$\Omega_g \sim \left(\frac{h}{H_0 P} \right)^2; \quad (4.1)$$

for $h = 10^{-13}$ this gives unity for $P \simeq 30,000$ sec. This estimate encourages us to proceed with a more accurate analysis, taking into account also the possibility of exploiting the peculiar nature of the signal.

Even if several standard relativistic cosmologies, as largely discussed in the literature (see, e.g., Matzner 1968, Thorne 1987, Grishchuk 1988), include an isotropic GW background, very little can be said about its spectral distribution, due to our incomplete knowledge of the primordial Universe. Indeed, the experimental analysis of the physical conditions present in the very early Universe is one of the main task of the not-yet-born *Gravitational Astronomy*.

A remarkable exception to this rather gloomy statement can be found in inflationary cosmologies. In fact, predictions by these models are very precise, in terms of the resulting GW power spectrum (Starobinsky 1979). However, the conclusions that can be drawn from several works in this field indicate that the spectral distribution is strongly dependent on the inflationary mechanism assumed. For example, for power-law inflation, S_ρ turns out to have more power on larger wavelengths than for purely exponential inflation (Sahni 1990).

On the other hand, in order to dig into the noise we have to assume a reasonable form of the power spectrum and scan the experimental data using the typical structures of the function (in our case the autocovariance $C(t)$) that we use in the statistical analysis. We will assume, for convenience, that the energy density spectrum is given by a power law of arbitrary index, i.e.

$$S_\rho(\omega) = k \omega^\alpha. \quad (4.2)$$

Obviously, equation (4.2) can not hold in the whole frequency range $(0, \infty)$, since the resulting total energy would be infinite. In other words, besides equation (4.2), we must also assume the existence of a physical cut-off Γ , in the lower or upper region according to the sign of $1 + \alpha$, in order of having a finite energy density. It must be said that inflationary models are the only ones able to relate these cut-offs to physical effects, even if the high frequency part of the relic graviton spectrum is rather sensitive to the details of the phase transition (Allen 1988). We will not make any hypothesis on the position of these cut-offs, apart from requiring that equation (4.2) holds within our observational window (ω_1, ω_2) .

In general, even with this simplifying assumptions, it is not possible to calculate analytically the autocovariance function $C(t)$. Here, we will focus our attention on two remarkable cases, corresponding to $\alpha = 2$ and $\alpha = 0$.

4.1 A flat amplitude spectrum.

If we assume that

$$S_h(\omega) = \text{crest.} \propto \alpha = 2 \quad (4.3)$$

then we are able to compute analytically $C(t)$. By using equations (3.4) and (4.3) we find¹

$$\langle H(t) \rangle_\phi = \frac{\langle h^2 \rangle}{8} \delta(t), \quad (4.4)$$

where $\delta(0) = 1$. The evaluation of the first three terms in equation (3.6) is immediate, while $I(t)$ may be explicitly calculated via equation (3.7) to give

$$I(t) = \frac{\langle h^2 \rangle}{4\ell^3} (2\ell - t)(t - \ell)\Theta(2\ell - t). \quad (4.5)$$

Therefore, the autocovariance function, for non-negative times, reads

$$C(t) = \frac{\langle h^2 \rangle}{2} \left[\delta(t) - \frac{1}{6} \delta(t - 2\ell) + \frac{1}{2} \frac{(2\ell - t)(t - \ell)}{\ell^3} \Theta(2\ell - t) \right]. \quad (4.6)$$

Figure 1 shows the autocorrelation function, i.e. $C(t)$ normalized to the value at the origin. The main feature of this function is the negative peak at $t = 2\ell$, of amplitude

$$C(2\ell)/C(0) = -1/6, \quad (4.7)$$

which is a direct consequence of the sinusoidal modulation of S_y ($S_y \propto \mathbf{R}$). Moreover $C(t) = 0$ for $t > 2\ell$, while in the range $0 < t < 2\ell$ we have only the weak contribution

¹In deriving equation (4.4) we have assumed $(\omega_1, \omega_2) \rightarrow (0, \infty)$, and normalized the result according to equation (3.5).

from $I(t)$, given by equation (4.5).

4.2 A flat energy spectrum.

The calculations presented in §4.1 are based on the only assumption which allows a simple analytical treatment of the autocovariance function. However, from physical arguments, one is tempted to exclude the case $\alpha = 2$, due to the steep increase of S_ρ as ω^2 . A more reasonable choice could be

$$S_\rho(\omega) = k = \text{const.} \quad \text{for } \alpha = 0 \quad (4.8)$$

within our experimental frequency range. As shown in Appendix A, the time derivative of $C(t)$ is then given by

$$\frac{dC}{dt} = \begin{cases} -\frac{2\pi k}{3} \left[1 + \left(5 - \frac{2t}{\ell} \right) \left(1 - \frac{t}{\ell} \right)^2 \right] & (0 < t < 2\ell), \\ 0 & (\forall t > 2\ell). \end{cases} \quad (4.9)$$

Thus, $C(t)$ has a flex point at $t = \ell$ and becomes constant for lags greater than the RTLT. Note the discontinuity of its derivative at $t = 2\ell$ (see figure 2). The constant value of $C(t)$ for $t > 2\ell$ is different from zero, and has to be calculated numerically. This characteristic of $C(t)$ turns out to be very important when looking for the best data analysis strategy, as discussed in the following section.

5 Data Analysis Strategies

Fundamentally, in past and present Doppler search for a GW background, three different methods have been used, all of them based on the study of the autocovariance function. We will analyze them in detail.

5.1 First method.

This method has been applied by Anderson & Mashhoon (1985) on the *Pioneer 10* data, and is essentially based on the variance of the Doppler data. From equations

(2.14) and (3.9) we have

$$\sigma_y^2 \equiv C(0) = 8 \int_{\omega_1}^{\omega_2} d\omega \cdot \frac{R(\omega\ell) S_\rho(\omega)}{\omega^2}. \quad (5.1)$$

If we limit our search in the low frequency region ($\omega\ell \ll 1$), then we can use the approximate expression (2.12) for R , obtaining

$$\sigma_y^2 \simeq \frac{64}{15} \pi \ell^2 \rho_g. \quad (5.2)$$

Here ρ_g represents the contribution to the energy density of the Universe coming from the low frequency GW ($\omega_1 \leq \omega \ll 1/\ell$). In terms of the density parameter Ω_g , we can rewrite equation (5.2) as (we assume here $H_0 = 75 \text{ Km sec}^{-1} \text{ Mpc}^{-1}$)

$$\Omega_g \simeq 1 \times 10^{35} \left(\frac{\sigma_y}{\ell(\text{sec})^2} \right)^2. \quad (5.3)$$

Thus, this method provides an upper limit for Ω_g without any hypothesis on S_ρ , since what we get is already an integrated quantity. On the other hand, it presents some practical problems. First, since all sources of noise contribute to $C(0)$, we can not discriminate between them. Secondly, it can be applied only in the low frequency region, thus requiring long periods of observations, and without any clue regarding how to extrapolate the obtained estimate to the upper part of the spectrum. Moreover, unless one has a considerably long record of data, the number of experimental points which one is considering can be dangerously small from a statistical point of view. Finally, we must also remember that sometimes the pre-processing procedure of the real Doppler data, explained in great detail in several papers (see, e.g., Bertotti *et al.* 1992?), is, in a sense, equivalent to a high-pass filter, implying an estimate (5.3) too optimistic.

5.2 Second method.

Hellings and collaborators (Hellings 1981, Hellings *et al.* 1981) have proposed a slightly more complex method, based on the assumption of a constant spectrum of $\langle h^2 \rangle$. Therefore, in this section we shall make use of the calculations presented in §4.1. In particular, they suggest looking for the negative peak of the autocovariance function at the RTIT, which, from equations (4.6) and (4.7), amounts to

$$C_g(2\ell) = -\frac{\langle h^2 \rangle}{12}. \quad (5.4)$$

Since this peak, if present, is buried into the noise, they assume that the sensitivity is dictated by the statistical noise, given by (Jenkins & Watts, 1968)

$$\sigma_c^2(t) = \frac{1}{u^2} \int_{-u}^u d\tau (u - |\tau|) [C;*(\tau) + L'(\tau + t)C(\tau - t)] \Big|_{T_1 \gg 1} \approx \frac{\langle y^2 \rangle^2}{T_1}, \quad (5.5)$$

where $u = T_1 - t$. In other words, one can estimate the quantity $\langle h^2 \rangle$ with the smallest among $C(0)$ and $6\sigma_c(2\ell)$, where $\sigma_c(2\ell)$ is the standard deviation of the autocorrelation function around the RTIT. Repeating this procedure with different sampling times Δt , corresponding to different upper frequencies ($\omega_2 = \pi/\Delta t$), one has the possibility of making a linear fit, since we have assumed $\langle h^2 \rangle \propto \omega_2$. The slope of this linear interpolation provides the (constant) value of S_h , and thus, from equation (2.7), the value of S_ρ , which can be integrated over the frequency range to give the estimated upper limit of ρ_g .

Also this method requires some comments. Even if, in general, increasing the sampling time we get a lower $\sigma_c(2\ell)$, we are not guaranteed, a priori, that this relationship be linear. For example, for the particular set of *Voyager I* data analyzed by Hellings *et al.* (1981), one finds $\langle h^2 \rangle \propto \ln(\omega_2/\omega_1)$, implying $S_h \propto \omega$, which contradicts the hypothesis (4.3). Since that hypothesis has been utilized when multiplying $\sigma_c(2\ell)$ by 6, one could easily overcome this problem. Substituting 6 with the Col'met factor, once determined the real dependence of S_h on ω . To be more precise, we have plotted, in

figure 3, the value of the autocorrelation function at $t = 2\ell$, as a function of the spectral index α . As one can see, the error made by Hellings *et al.* is less than 20%, but one would get very different results if redder spectra were considered.

We propose to modify the previous method in the following way. From equation (2.14) we see that, when S_h is constant, S_y is proportional to the filter \mathbf{R} . This, in turn, is well approximated by a sinusoidal function for frequencies above $1/J!$ (see eq. (2.12), and Estabrook & Wahlquist 1975). Therefore, the search of the GW background, with the assumed spectral index $\alpha = 2$, reduces to the search of sinusoidal signal, of ‘Known ‘pulsation’ 2ℓ , in the ‘time’ sequence represented by the Doppler power spectrum S_y . This kind of analysis is very common in astronomy, for example in the search for X-binaries.

The first step consists in taking the power spectrum of the data which should contain the sinusoidal signal, i.e. $S_y(\omega)$, and then to look for a peak in the expected channel, corresponding to the lag $\tau = 2\ell$. Recalling equation (3.9), we will thus consider the function

$$\mathcal{A}(t) \equiv \left(\frac{C(t)}{\sigma_c} \right)^2, \quad (5.6)$$

where σ_c is the standard deviation of the autocovariance function. As we shall now see, this normalization simplifies the statistical properties of \mathcal{A} , when the noise is normally distributed. In fact, if $y(t)$ is a gaussian noise with zero average and unit variance (see fig. 4a and 4b), then its power spectrum S (fig. 4c) is distributed as a χ^2 function with two degrees of freedom, or

$$f(S) = e^{-S} \quad (5.7)$$

Figure 4d shows the periodogram of the spectral lines of S , together with the χ^2 function (5.7). Since the autocovariance function is also normally distributed, one can easily show that the distribution function of \mathcal{A} (fig. 4e) is a χ^2 with one degree of freedom,

i.e.

$$f(\mathcal{A}) = \frac{1}{\sqrt{2\pi}} e^{-\mathcal{A}^2/2} . \quad (5.8)$$

In particular, its average is $\mu = 1$ and its variance is $\sigma^2 = 2$. Figure 4f shows the probability distribution of \mathcal{A} , together with the expected distribution (5.8). Note that the functions (5.7) and (5.8) have no free parameters, being by definition normalized to one.

Setting a threshold condition \mathcal{A}_{det} for the autocovariance function - which can be done using well known statistical techniques - one can assert the detection of the gravitational signal with a given confidence level if $\mathcal{A}(2\ell) > \mathcal{A}_{det}$; otherwise (and this is the case we are usually dealing with) it is only possible to give an upper limit.

Following Hellings *et al.*, but taking into account the previous remarks, we compute the upper limit on $\langle h^2 \rangle$ using (5.4) and (5.6)

$$\langle h^2 \rangle = 12\sigma_c \sqrt{\mathcal{A}(2\ell)} , \quad (5.9)$$

and repeat this procedure for different values of the sampling time Δt . Then we check that the relation between $\langle h^2 \rangle$ and $1/\Delta t$ is linear, in order to ensure the consistency of the analysis with the hypothesis $S_h = const.$, and eventually, from the slope of this linear function, we deduce the constant value of S_h , which gives, after a trivial integration, the upper limit on ρ_g .

5.3 Third method.

The last method assumes the hypothesis $S_\rho = const.$ over the experimental bandwidth (ω_1, ω_2) . Thus all the equations of section 4.2 apply in this case. In particular, we have seen that the autocovariance function $C(t)$ takes a *non zero constant* value for lags greater than the RTLT (see equation (4.9)); we are going to exploit this feature to set an upper limit on the energy content of the gravitational background.

As in the previous section we shall use the normalized function \mathcal{A} , defined by equa-

tion (5.6). Its statistical properties have been thoroughly investigated in the previous subsection.

We also indicate with \mathcal{A}_g the constant GW contribution to $\mathcal{A}(t)$ for $t > 2\ell$. Of course, the autocovariance function $C(t)$ fails to become exactly constant, due to the presence of noise. Apart from statistical noise, the main contribution, for $t > 2\ell$, comes from the plasma and the troposphere (Hellings 1981). Regarding the latter, it is possible to show that $C_n(t) \sim t^{-1/3}$ for $t \gg 2\ell$. The plasma contribution is more complicated, since its effect is distributed along the whole light path, not just at the beginning and the end. However it can be shown having an analogous decreasing behavior as t increases. For more details, see Appendix B, where the contributions of the troposphere and plasma noise to the autocovariance function are analytically computed in the limit $t \gg 2\ell$.

Thus, we can set an upper limit to \mathcal{A}_g taking the average of $\mathcal{A}(\tau)$ over the interval $2\ell < \tau < \tau_{\max}$, where τ_{\max} is the maximum allowed value for τ , i.e.

$$\mathcal{A}_g \lesssim \langle \mathcal{A} \rangle = \frac{1}{\tau_{\max} - 2\ell} \int_{2\ell}^{\tau_{\max}} d\tau \mathcal{A}(\tau). \quad (5.10)$$

In an ideal experiment, τ_{\max} is simply determined by the duration T_1 of the observations. Unfortunately, in practice the extraction of the real time series from the raw data involves a complex procedure, described elsewhere (Bertotti *et al.* 1992), which strongly affects the low frequency region of the spectrum. Therefore, one should first look at the power spectrum of the whole passage, and then carefully decide where to locate the minimum frequency, or equivalently τ_{\max} .

Finally, the upper limit \mathcal{A}_g is numerically related to an upper limit on the (assumed) constant S_ρ through the equation

$$S_\rho = \left| \frac{\sigma_c \sqrt{\mathcal{A}_g}}{8 \int_{\omega_1}^{\omega_2} d\omega \frac{\mathbf{R}(\omega\ell) \cos 2\omega\ell}{\omega^2}} \right|. \quad (5.11)$$

The total energy content of the gravitational background in the experimental band

width $h(\omega_1, \omega_2)$ is thus given by

$$\rho_g = \frac{(\omega_2 - \omega_1)}{\pi} S_\rho. \quad (5.12)$$

In order to test the compatibility of the hypothesis $S_\rho = \text{const.}$ with the data set, a safe way to proceed is to repeat the whole procedure sampling the data at different rates, and compare the resulting energy densities ρ_g . The consistency of this method requires that ρ_g increases linearly with the sampling rate $1/\Delta t = \omega_2/\pi$, or, in other words, that S_ρ , as given by equation (5.11), remains approximately constant.

6 Conclusions

We complete our work with a brief comment regarding the expected results from the three methods presented here. As we said, the first method usually gives good, i.e. low, upper limits, as a consequence of various systematic effects. Even if these limits are presumably higher than the expected values for ρ_g , one cannot consider them as truly conservative, in the sense that a considerable fraction of signal could be rejected during the data analysis.

Regarding the last two methods, their conservative quality is obtained to the cost of their weakness. In other words, the upper limits obtained with methods 2 and 3 are valid if and only if the underlying assumptions about the spectral slope of the signal ($\alpha = 2$ in the first case, $\alpha = 0$ in the second one) are true. However, it sounds reasonable to believe that the upper limits obtained with these hypotheses remain valid also for more general spectra than those considered here. Hopefully, in the near future, the detection of a GW background in some region of the frequency spectrum, presumably above the Doppler range, will give us a clear indication about the spectral properties of the signal to be searched for with a Doppler experiment.

Among the three methods described, the last one is certainly the most promising. In fact, as we have seen, the upper limit on ρ_g is obtained, in this case, through an average of the autocovariance function over a large number of points above the RTF. Since the main deterministic sources of noise do not contribute considerably to this

part of the autocovariance function, one is expecting a sharp decrease in the stochastic noise level as the average is performed.

In this paper we have considered only the case of a single experiment. In principle, the unknown stochastic nature of the GW background makes it impossible to claim a safe detection in a single spacecraft experiment. This fact suggests us to perform, when possible, coincidence experiments, where a cross-correlation between the outputs could allow the extraction of a common signal from various independent noises. An experiment of this kind has been performed during last spring, when the three spacecraft *Galileo*, *Mars Observer*, and *Ulysses* had been continuously and simultaneously tracked for two weeks.

Acknowledgements

This work is a contribution to the *Ulysses* Gravitational Wave Experiment, and could never have been written without the participation of the whole team. We are grateful, in particular, to the Principal investigator Prof. B. Bertotti, for having stimulated and supported our work. We also thank J.D. Anderson, J.W. Armstrong, R.W. Hellings, J.J. Less, and H.D. Wahlquist for their comments and help. We would like to thank the Italian MURST for financial support. G.G. did part of this work at JPL, while he held a National Research Council/JPL Research Associateship.

Appendix A

From equation (2.7), with $S_\rho = k$, we get $S_h(\omega) = 16\pi k\omega^{-2}$, and therefore equation (3.4) gives (see also note in §4.1)

$$\frac{d\langle H(t) \rangle_\phi}{dt} = -2\pi k [\Theta(t) + \lambda], \quad (\text{A.1})$$

where λ is an arbitrary constant. From equation (3.6) we thus find

$$\frac{dC}{dt} = -8\pi k \left[\Theta(t) + \frac{1}{6}\Theta(t - 2\ell) + \frac{1}{6}\Theta(t + 2\ell) + \frac{2}{3}\lambda + \frac{dI}{dt} \right]. \quad (\text{A.2})$$

The derivative of $I(t)$ is easily found from equation (3.7), since all we have to do is to modify the integration limits according to the argument of the Heaviside function. The result is

$$\frac{dI}{dt} = \frac{8\pi k}{3} \left[\Theta(t) + \Theta(t - 2\ell) + \Theta(2\ell - t) - \frac{5}{4} \left(5 - \frac{2t}{\ell} \right) \left(1 - \frac{t}{\ell} \right)^2 \right] + 2\lambda \quad (\text{A.3})$$

Inserting equation (A.3) in equation (A.2) we eventually find

$$\frac{dC}{dt} = \begin{cases} -\frac{2\pi k}{3} \left[1 + \left(5 - \frac{2t}{\ell} \right) \left(1 - \frac{t}{\ell} \right)^2 \right] & (0 < t < 2\ell), \\ 0 & (w > 2\ell), \end{cases} \quad (\text{A.4})$$

independently from the value of the arbitrary constant λ .

Appendix B

Here we calculate the behaviour of the autocovariance function $C(t)$ for the troposphere and plasma noise for lags greater than the RFLT.

The theoretical expressions $C_T(t)$ and $C_P(t)$ has been derived by Hellings (1981) (equation [47]):

$$C_T(t) = \frac{9\Gamma\left(\frac{1}{3}\right)}{10(\Delta t)^2} t_0 f(2\ell, t, \Delta t), \quad (\text{B.1})$$

$$C_P(t) = \frac{9\Gamma\left(\frac{1}{3}\right)}{10(\Delta t)^2} p_0 \int_{R_0}^R \frac{f[2(r - R_0), t, \Delta t]}{r^4} dr, \quad (\text{B.2})$$

where t_0 and p_0 are the reference levels of the troposphere and plasma noise power spectrum, Δt is the sampling time and R and R_0 are the heliocentric distances of the spacecraft and of the earth. The function $f(x, t, \Delta t)$ is:

$$\begin{aligned} f(x, t, \Delta t) = & \frac{1}{4} |x + t - \Delta t|^{5/3} + \frac{1}{4} |x - t + \Delta t|^{5/3} \\ & + \frac{1}{4} |t + \Delta t - x|^{5/3} + \frac{1}{4} |x + t + \Delta t|^{5/3} \\ & + \frac{1}{2} |t + \Delta t|^{5/3} + \frac{1}{2} |t - \Delta t|^{5/3} \\ & - \frac{1}{2} |x + t|^{5/3} - \frac{1}{2} |x - t|^{5/3} - |t|^{5/3} \end{aligned} \quad (\text{B.3})$$

Expanding $f(x, t, \Delta t)$ for $t \gg 2\ell$ (i.e. $t \gg x \pm \Delta t$ because $x \leq 2\ell$ and $\Delta t \ll 2\ell$) to the second order in $(x \pm \Delta t)/t$, x/t and $\Delta t/t$, we have:

$$f(x, t, \Delta t) = \frac{10}{9} (\Delta t)^2 t^{-1/3} + O(t^{-4/3}). \quad (\text{B.4})$$

From equations (B.1), (B.2) and (B.4) the asymptotical expressions of the autocovari

ance functions become:

$$C_T(t) = \sqrt{3}\Gamma\left(\frac{1}{3}\right)t_0t^{-1/3}[1 + O(t^{-1})], \quad (\text{B.5})$$

and

$$C_P(t) = \frac{\sqrt{3}}{3}\Gamma\left(\frac{1}{3}\right)\left(\frac{1}{h_0^3} - \frac{1}{h^3}\right)p_0t^{-1/3}[1 + O(t^{-1})]. \quad (\text{B.6})$$

References

- ALLEN, B. 1988, *Phys. Rev.*, **D37**, 2078.
- ANDERSON, J.D., & MASHHOON, B. 1985, *Astrophys. J.*, **290**, 445.
- BERTOTTI, B., AMBROSINI, R., ASMAR, S.W., BRIENKLE, J.P., COMORETTO, G., GIAMPIERI, G., IESS, L., MESSERI, A., & WAHLQUIST, H.D. 1992, *Astron.Astrophys. Suppl. ser.*, **92**, 431.
- BERTOTTI, B., AMBROSINI, R., ASMAR, S.W., COMORETTO, G., GIAMPIERI, G., IESS, L., KOYAMA, Y., MESSERI, A., VECCHIO, A., & WAHLQUIST, H.D. 1994, *paper in preparation*.
- CARR B. J. 1980, *Astron. Astrophys.*, **89**, 6.
- ESTABROOK, H. H., & WAHLQUIST, H.D. 1975, *Gen. Rel. Grav.*, **6**, 439.
- GIAMPIERI, G. 1992, *Ph.D. Thesis*, (University of Pavia, unpublished).
- GRISHCHUK, L.P. 1988, *Sov. Sci. Rev. E. Astrophys. Sp. Phys.*, **7**, 267.
- HELLINGS, R.W. 1981, *Phys. Rev.*, **D23**, 832.
- HELLINGS, R. W., CALLAHAN, P. S., & ANDERSON, J.D. 1981, *Phys. Rev.*, **D23**, 844.
- ISAACSON, R. A. 1968, *Phys. Rev.*, **166**, 1272.
- JENKINS, G. M., & WATTS, D. G. 1968, *Spectral Analysis and Its Applications*, (Holden-Day, San Francisco).
- MATZNER, R.A. 1968, *Astrophys. J.*, **154**, 1123.
- SAHNI, V. 1990, *Phys. Rev.*, **D42**, 453.
- STAROBINSKY, A.A. 1979, *JETP Lett.*, **30**, 682.
- THORNE, K. S. 1987, in *300 Years of Gravitation*, ed. S.W. Hawking (Cambridge University Press, Cambridge).

Figure Captions

Figure 1

Autocorrelation function, $C(t)/C(0)$, for $\alpha = 2$. Time is expressed in units of RTI/T .

Figure 2

Autocorrelation function, $C(t)/C(0)$, for $\alpha = 0$. Time is expressed in units of RTI/T .

Figure 3

The autocorrelation function at $t = 2\ell$, as a function of the spectral index α . The dashed line represents the value $1/6$, which corresponds to $\alpha = 2$ (see equation (4.7)).

Figure 4

Statistical properties of a gaussian signal. (a) randomly generated gaussian noise y , (b) its distribution function, with $\mu \simeq 0$ and $\sigma \simeq 1$. (c) power spectrum S_y of y , (d) its spectral distribution. (e) our function \mathcal{A} , (f) its distribution function. In figures (b), (d), and (f), the abscissa 'Amplitude' represents the line amplitude in unit of standard deviation. The dashed lines in figures (d) and (f) represent, respectively, the theoretical functions (5.7) and (5.8).

Figure 1

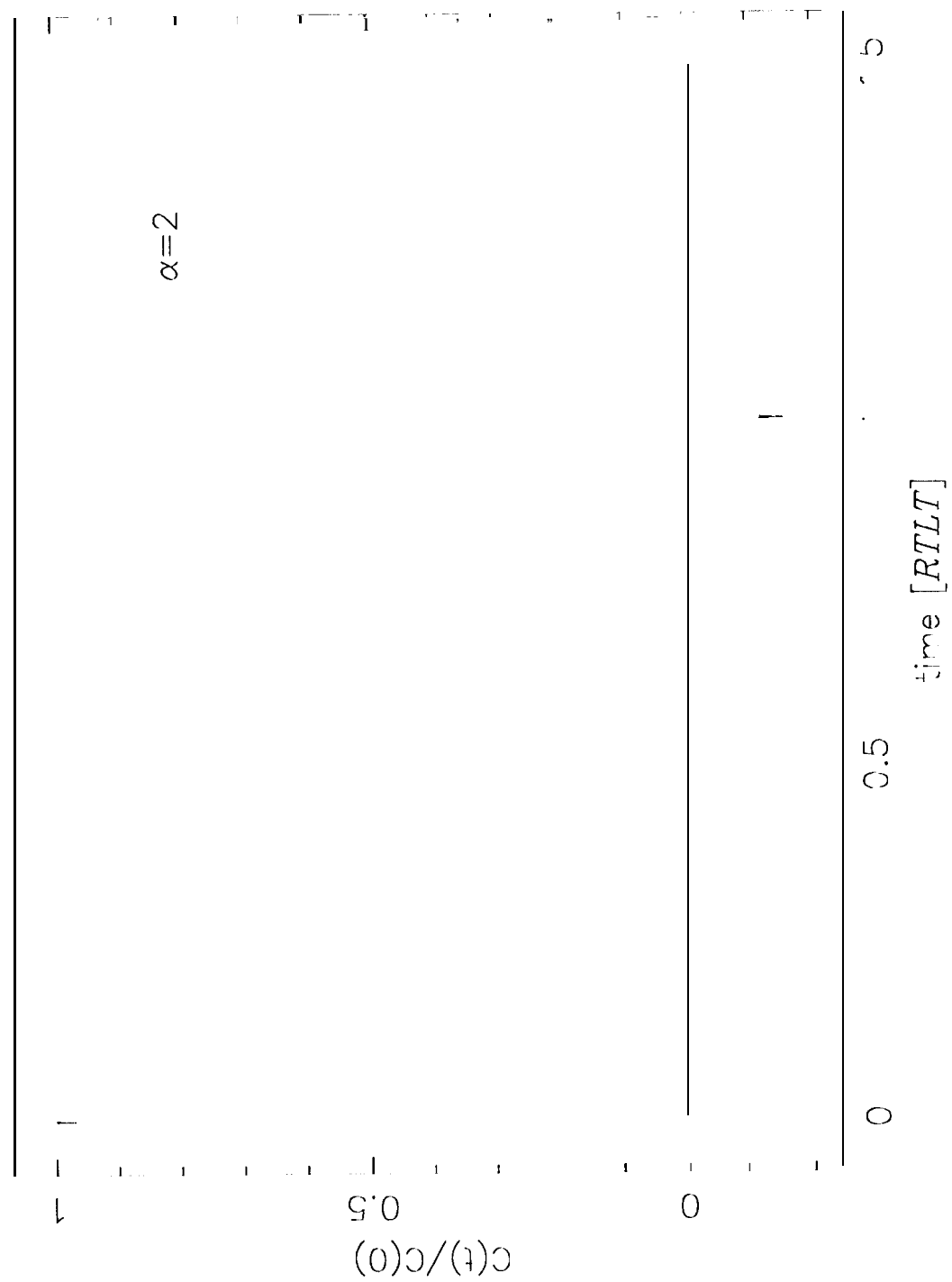


Figure 2

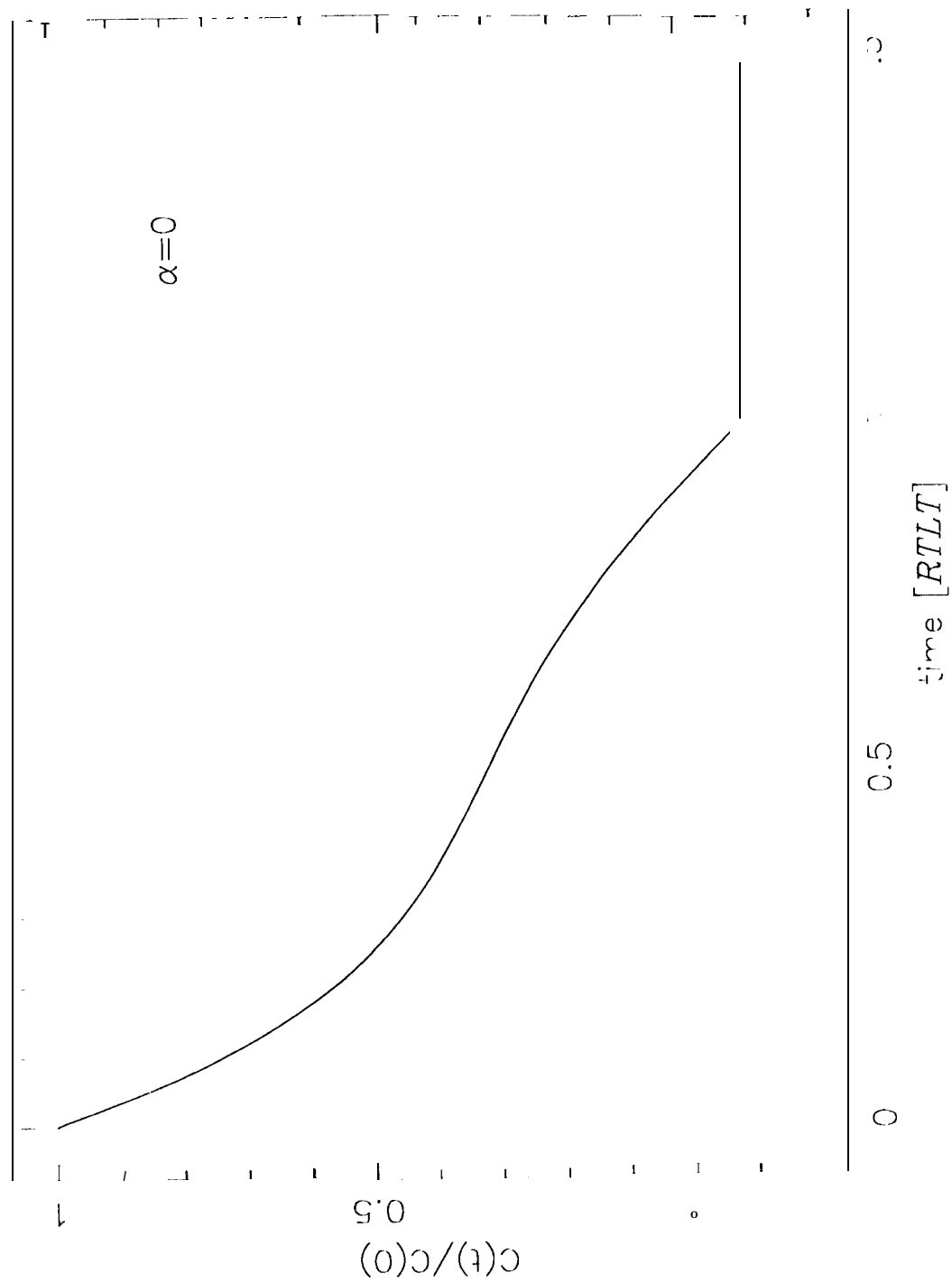
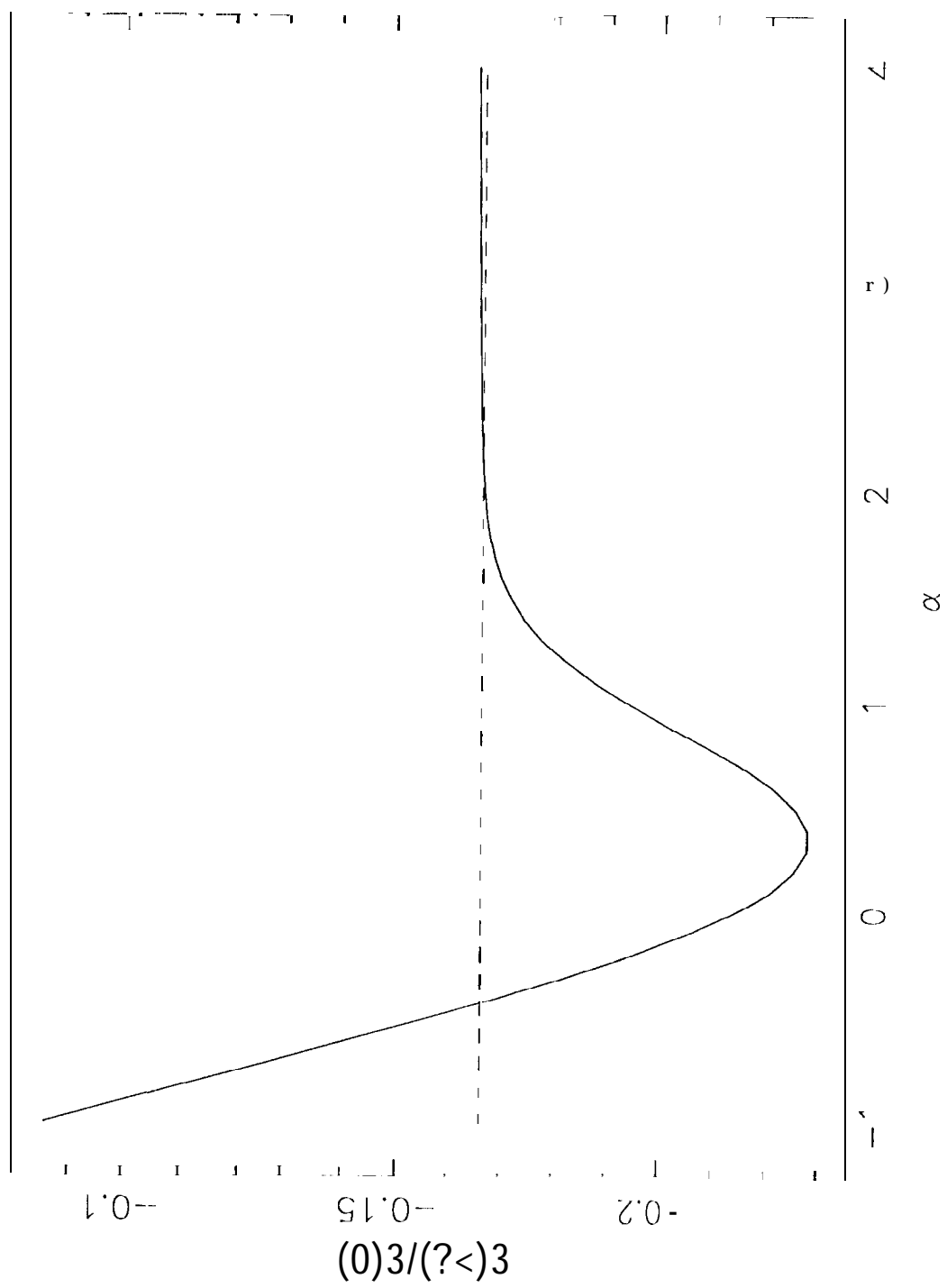


Figure 3



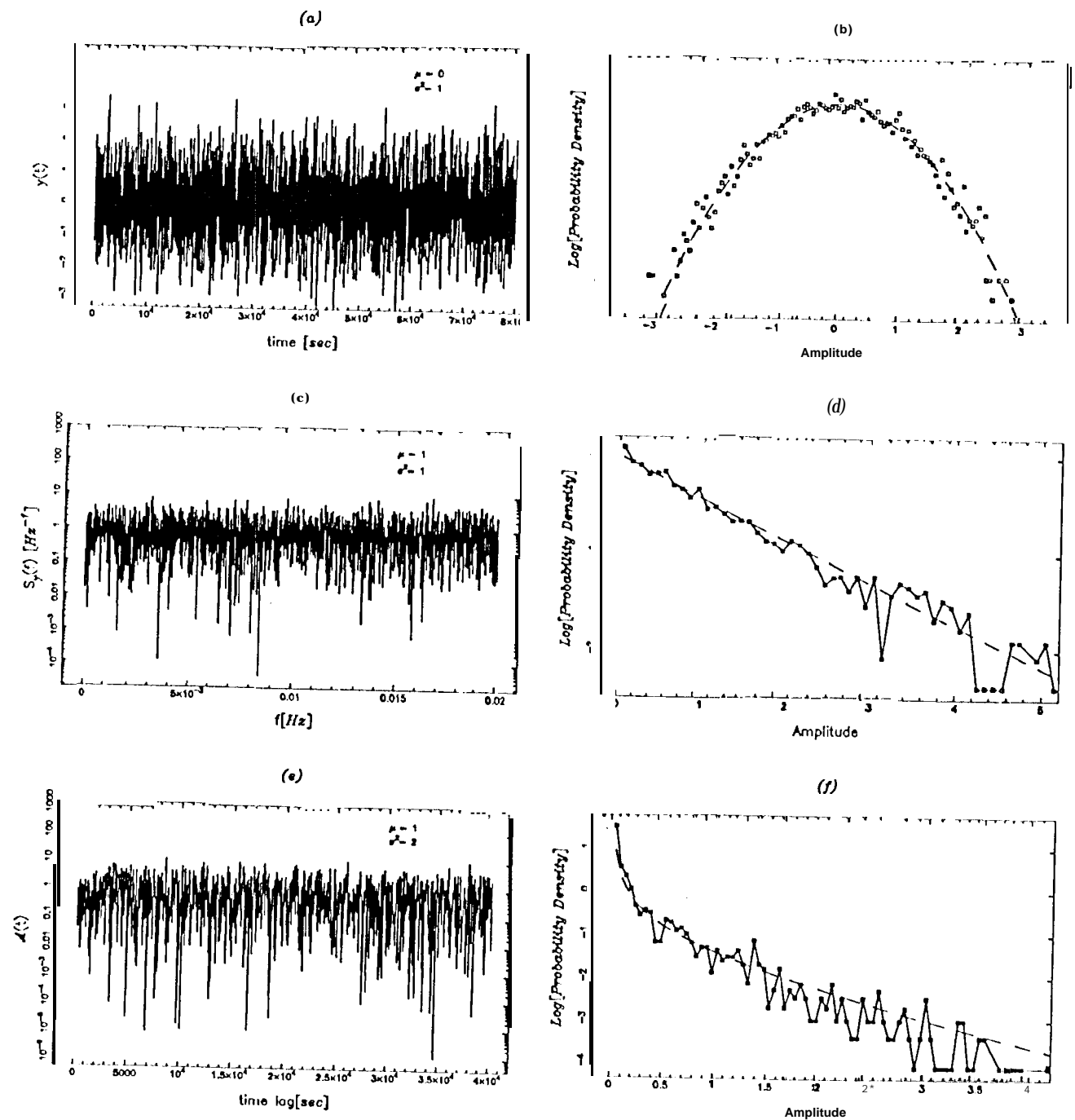


Fig. 4